



0008-8846(94)00117-0

SODIUM PHOSPHATE-DERIVED CALCIUM PHOSPHATE CEMENTS

Toshifumi Sugama and N.R. Carciello
 Energy Efficiency and Conservation Division
 Department of Applied Science
 Brookhaven National Laboratory
 Upton, New York 11973

(Refereed)

(Received November 29, 1993; in final form September 30, 1994)

ABSTRACT

Calcium phosphate cements (CPC) were synthesized by the acid-base reaction between sodium phosphate, NaH_2PO_4 or $-(\text{-NaPO}_3)_n$, as the acid solution, and calcium aluminate cements (CAC) as the base reactant at 25°C . The extent of reactivity of $-(\text{-NaPO}_3)_n$ with CAC was much higher than that of NaH_2PO_4 , thereby resulting in a compressive strength of > 20 MPa. Sodium calcium orthophosphate (SCOP) salts as amorphous reaction products were responsible for the development of this strength. When this CPC specimen was exposed in an autoclave, in-situ amorphous \rightarrow crystal conversions, such as $\text{SCOP} \rightarrow$ hydroxyapatite (HOAp), and $\text{Al}_2\text{O}_3 \cdot x\text{H}_2\text{O} \rightarrow \gamma\text{-AlOOH}$, occurred at $\approx 100^\circ\text{C}$, while the rate of reaction of the residual CAC with the phosphate reactant was increasingly accelerated by hydrothermal catalysis. Based upon this information, we prepared lightweight CPC specimens by hydrothermally treating a low-density cement slurry (1.28 g/cc) consisting of CAC powder, $-(\text{-NaPO}_3)_n$ solution, and mullite-hollow microspheres. The characteristics of the autoclaved lightweight specimens were a compressive strength of > 9.0 MPa, water permeability of $\approx 5.0 \times 10^{-3}$ milli darcy, and a low rate of alkali carbonation. The reasons for such a low carbonation rate reflected the presence of a minimum amount of residual CAC, in conjunction with the presence of HOAp and $\gamma\text{-AlOOH}$ phases that are unsusceptible to wet carbonation.

Introduction

We reported^{1,2} that hydrothermally synthesized calcium phosphate cements (CPC) with a phase composition of hydroxyapatite, $\text{Ca}_5(\text{PO}_4)_3(\text{OH})$, and boehmite, $\gamma\text{-AlOOH}$, have a high potential for use as alkali carbonation-resistant cementing materials to support intermediate casing pipe, and also to protect the casing from corrosive fluids and gases in the geothermal wells where temperatures may rise to 300°C . The crystalline phases responsible for CO_2 -resistance were assembled by hydrothermally catalyzed in-situ phase-transformation of amorphous $\text{NH}_4\text{CaPO}_4 \cdot x\text{H}_2\text{O}$ and $\text{Al}_2\text{O}_3 \cdot x\text{H}_2\text{O}$ compounds derived from an acid-base reaction at room temperature between the ammonium dihydrogen phosphate ($\text{NH}_4\text{H}_2\text{PO}_4$)-based fertilizer as acid reactant, and commercial calcium aluminate cements (CAC) as base reactants. Although the rate of carbonation depended mainly on the chemical ingredients of CAC, the CPC specimens which had well-formed hydroxyapatite and

boehmite crystalline phases yielded only 0.2 % CaCO_3 after exposure for 120 days to Na_2CO_3 -laden water at 250°C . Such promising results encouraged us to develop new formulations for CPC-based material systems which can be used to complete geothermal wells. One important consideration in designing a well-cementing slurry is that it should be lightweight, because the use of slurries of normal density, 1.9 to 2.0 g/cc, for completing geothermal wells frequently creates lost circulation zones, which are caused by the formation of voids in the underlying rocks during drilling operations. In other words, when attempts are made to cement the well in weak, unconsolidated rock zones with very fragile gradients, these unconsolidated formations fracture from the significant hydrostatic pressures required to pump the highly dense cement slurries. To avoid this problem, low-density cement slurries are needed. In preparing such a lightweight slurry, our preliminary experiments suggested that incorporating into the CPC slurry aluminosilicate-base hollow microspheres, with a density of 0.67 g/cm³ and a particle size of 75 to 200 μm , conferred such suitable properties, so that the slurry had a low density of ≈ 1.3 g/cc and a compressive strength greater than 6.9 MPa for 200°C -autoclaved specimens³.

On the other hand, environmental and health concerns are still the most important factors for the producers of well cements. In considering the use of environmentally benign materials, $\text{NH}_4\text{CaPO}_4 \cdot x\text{H}_2\text{O}$ may be unsuitable as the acid reactant, because of the emission of NH_3 gases during the hydrothermally catalyzed processing of CPC. Thus, we focused our emphasis on eliminating any environmental problems in making lightweight CPC slurries.

Commonly, the M species in the dihydrogen-based phosphate acid reactants, MH_2PO_4 , corresponds to NH_4 , Na, K, and Li. Thus, all of the alkali metal-containing phosphate compounds are considered as the environmentally safe reactants. In this study, we selected the Na-phosphate compounds, such as sodium phosphate, monobasic, NaH_2PO_4 , and sodium polyphosphate, $\text{-(NaPO}_3\text{)-}_n$, as the acid reactants, so that alternative materials are available if, at some future time, the $\text{NH}_4\text{H}_2\text{PO}_4$ becomes environmentally unacceptable to regulatory agencies. Our experimental evaluation of the ability of Na-phosphate reactants to produce CO_2 -resistant lightweight CPC involved examining the changes in porosity, compressive strength, and phase composition for the neat cement pastes as a function of hydrothermal temperatures up to 300°C . These data were correlated directly to the properties of the aluminosilicate hollow microsphere-filled lightweight CPCs, such as water permeability, rate of alkali carbonation, and compressive strength.

Experimental

Materials

The commercial calcium aluminate cement (Refcon) supplied by the Lehigh Portland Cement Company was used as the base solid reactant. The X-ray powder diffraction of this cement showed that its chemical component consisted of three major phases, monocalcium aluminate, $\text{CaO} \cdot \text{Al}_2\text{O}_3$, (CA), gehlenite, $2\text{CaO} \cdot \text{Al}_2\text{O}_3 \cdot \text{SiO}_2$, (C_2AS), and calcium dialuminate, $\text{CaO} \cdot 2\text{Al}_2\text{O}_3$, (CA_2). Two sodium phosphate reagents, monobasic (NaH_2PO_4) and polybasic $\text{-(NaPO}_3\text{)-}_n$, were dissolved in water to make 20, 30, and 40 wt% sodium phosphate solutions as the acid liquid reactants. The pHs of the 20, 30, and 40 wt% NaH_2PO_4 solutions were 4.21, 4.05, and 3.80, respectively, and the 20, 30, and 40 wt% $\text{-(NaPO}_3\text{)-}_n$ solutions corresponded to pH 6.40, 6.15, and 5.86, respectively. The commercial aluminosilicate-based hollow microsphere called Extendspheres (PQ Corp), were incorporated into the cement slurry as lightweight filler. These microspheres had a density of 0.67 g/cm³ and a particle size from 75 to 200 μm .

Neat cement pastes were prepared by thoroughly hand-mixing 60 wt% calcium aluminate cement (CAC) and 40 wt% sodium phosphate solution at room temperature; cement slurries were cast in cylindrical molds (30 mm-diam x 65 mm-long), and then left for 24 hrs at room temperature before autoclaving for 20 hrs at 100, 200, and 300°C . The composition of the low-density CPC slurry consisted of 40 wt%

CAC, 20 wt% microspheres, and 40 wt% sodium phosphate solution. The densities for all the lightweight slurries prepared from 1.25 to 1.28 g/cc at room temperature, while the original CPC slurry without the microspheres had a density of 1.98 g/cc. The lightweight CPC (LCPC) specimens for the strength and water permeability tests were prepared by first dry-mixing the CAC powder with the lightweight filler; then, sodium phosphate solution was added and the slurry was thoroughly hand-mixed for ≈ 3 min. Next, the LCPC slurry was cast into cylindrical molds of 30 mm-diam. x 65 mm-long to measure compressive strength, and into discs of 30 mm-diam. x 39 mm-long for determining the water permeability. The molds and discs were then exposed in an autoclave at 100, 200, or 300°C for 20 hrs. To obtain the rate of carbonation, the failed LCPC specimens after compressive strength tests were crushed to a size of < 0.1 mm, and then the powdered samples were immersed for 10 days in a 0.05 M Na_2CO_3 -laden water at 100, 200, or 300°C.

Measurements

A Fourier transform infrared (FT-IR) spectrophotometer (Model 1605; Perkin Elmer) was used to identify the chemical reaction products. The phase composition and transformation of neat CPC and of microsphere-filled CPC specimens as a function of hydrothermal temperatures were explored by x-ray powder diffraction (XRD). Quantitative data on the amount of CaCO_3 formed in the LCPC bodies after exposure to Na_2CO_3 solution was obtained by thermogravimetric analysis (TGA), and by the weight loss at which thermal decomposition of CaCO_3 occurs over the range 600 to 700°C⁴. The porosity of neat CPC specimens was determined by helium comparison pycnometry. A Ruska liquid permeameter was used to measure the water permeability of LCPC specimens; these measurements were made by determining the amount of water which passes through the discs under a pressure gradient of 2 atm. Compressive strength was tested on neat and LCPC specimens; the results given are the average value from three specimens.

Results and Discussion

Neat CPC pastes

In our first experiment, attention was focused on measuring porosity and the compressive strength of the Na phosphate monobasic, (Na-M)- and polyphosphate, (Na-P)-derived CPC pastes allowed to set at room temperature (25°C) for 24 hrs after mixing. Table 1 shows the changes in helium-induced porosity and compressive strength of the CPC specimens as a function of concentration of acid reactants.

Using Na-M, no setting was observed in the 20 wt% reactant-mixed CPC. Even though the 30 and 40 wt% concentrations showed some degree of setting, the compressive strengths of their neat specimens were too low to be measured. In contrast, the Na-P-derived CPC specimens clearly verified that the changes in

Table 1. Changes in Porosity and Compressive Strength of Na-M- and Na-P-Derived CPC Specimens as a Function of Concentration of Acid Reactants.

Acid reactant	Concentration of acid reactant, wt%	Porosity, %	Compressive strength, MPa
Na-M	20	-*	-*
Na-M	30	55.2	-**
Na-M	40	53.0	-**
Na-P	20	46.4	6.85
Na-P	30	37.6	17.47
Na-P	40	27.7	28.42

* no setting of specimens

** Too weak to be measured

porosity and strength depend primarily on the concentrations of reactant. The values for porosity conspicuously decreased with an increased concentration of the reactant; correspondingly, there was an increase in the strength of specimens. The CPC specimens prepared from 40 wt% reactant had the highest strength of 28.42 MPa. Such good mechanical behavior directly reflected their relatively low porosity of 27.7 %.

To substantiate our explanation of why the Na-P acid reactant has a better effect on the development of strength than Na-M at room temperature, we inspected the chemical reaction products derived from the acid-base interaction by FT-IR and XRD. Figure 1 illustrates FT-IR spectra over the two frequency ranges from 4000 to 2500 cm^{-1} and 1400 to 600 cm^{-1} for the CAC and Na-M powder reactants as control samples, and the 40 wt% Na-M-induced CPC specimens after being left for 24 hrs at 25°C. The IR spectrum of CAC (a) showed that the non-reactive CAC reactants have already been partially hydrated, because of the presence of a peak at 3430 cm^{-1} , reflecting an O-H stretching vibration in H_2O . The typical spectral structure of Na-M reactant consists of O-H stretching in hydrates at 3430 cm^{-1} , P-O-H stretching at 2920 cm^{-1} ⁵, the stretching mode of the P=O double bond at 1280 cm^{-1} , Na-cation vibration on its oxygen cage at 1160 cm^{-1} ⁶, ionic P-O stretching in H_2PO_4^- at the peaks in the frequency ranging from 1100 to 1030 cm^{-1} ⁷, and the P-O-H bending at peaks ranging from 990 to 850 cm^{-1} . Compared with those of these control samples, the spectral features of Na-M-derived CPC specimens (c) were characterized by the appearance of a new peak at 1110 cm^{-1} , and the disappearance of the peaks belonging to the ionic P-O and P-O-H groups, while the maintenance of the prominent peaks at 1014, 810, 680, and 640 cm^{-1} , belonging to non-reactive CAC, and of the shoulder band of Na^+ ions at 1160 cm^{-1} was evident. This new peak reveals the formation of typical orthophosphate (PO_4) groups¹ in the sodium calcium phosphate compounds, produced by acid-base

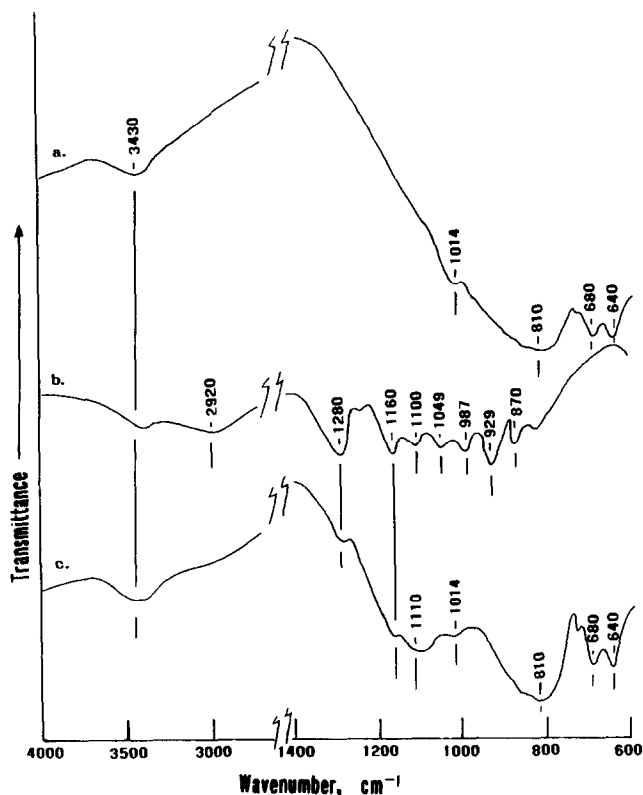
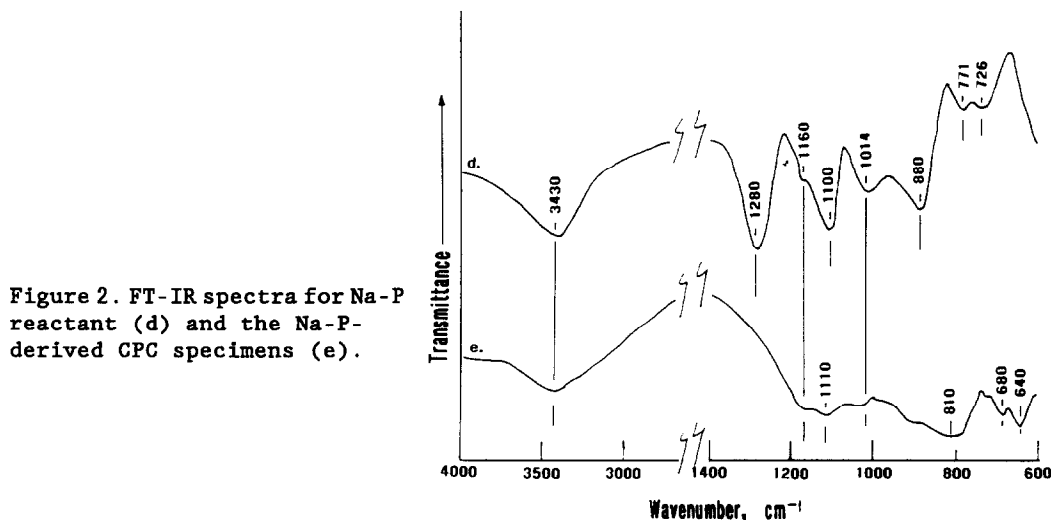


Figure 1. FT-IR absorption spectra for bulk CAC (a) and NaH_2PO_4 (b) reactants, and CPC specimens (c) prepared by mixing CAC powder and NaH_2PO_4 solution at 25°C.

reactions between CAC and Na-M. The O-H stretching band in the H_2O at 3430 cm^{-1} suggested that the hydrates not only reflect the partially hydrated CAC reactants, but may also be associated with the formation of sodium calcium orthophosphate (SCOP) hydrate salts, $\text{NaCaPO}_4 \cdot x\text{H}_2\text{O}$. Figure 2 shows the IR absorption bands of the Na-P reactant and the Na-P-derived CPC specimens. The spectral features of Na-P (d) represent the typical linear metaphosphate structure, reflecting the ionic P-O stretching vibration at the peaks of 1100 and 1014 cm^{-1} , the stretching mode of P-O-P bonds at 880 cm^{-1} , and its bending mode at the doublet in the $780\text{--}710\text{ cm}^{-1}$ region. When the 40 wt% Na-P solution was incorporated into the CAC, the differences between the spectrum (e) and that of the Na-M-derived CPC (see Figure 1, C) were as follows: (1) the absence of a frequency band at 1280 cm^{-1} originating from P=O double bonds, with the emergence of a new band at 1110 cm^{-1} , and the elimination of the ionic P-O and P-O-P bands, ranging from 1014 to 640 cm^{-1} . It is apparent from the first finding (1) that Na-P was transformed into the SCOP salt, having a tetrahedral phosphate structure formed by the rupture of P=O bonds in Na-P. The second result (2) strongly suggested that Na-P reacts more favorably with the CAC reactant than Na-M. Thus, such an extensive reaction that converted Na-P into the SCOP salts was the reason why the Na-P-derived CPC specimens had superior mechanical behavior and lower porosity compared to the Na-M-derived specimens. The XRD pattern (not shown) of these CPC specimens exhibited only the presence of non-reactive CAC reactants, denoting that the SCOP salts formed by acid-base reaction at room temperature are essentially an amorphous phase. The amorphous SCOP salts, as the major reaction products which bind the partly reacted and non-reactive CAC particles into a coherent mass, were responsible for the development of strength of CPC at ambient temperature.

Our next experiment was to investigate the changes in chemical state, phase composition, compressive strength, and porosity of the 40 wt% Na-M- and Na-P-derived specimens after exposure for 24 hrs in an autoclave at 100 , 200 , and 300°C . Figure 3 depicts the FT-IR absorption spectra for the autoclaved Na-M specimens. The resultant spectral structure at 100°C closely resembled that obtained at 25°C (see Figure 1-C), suggesting that SCOP salts were still present in the matrix of the 100°C -autoclaved CPC specimens containing some non-reactive particles. However, when the hydrothermal temperature was increased to 200°C , the specimens showed striking differences in spectral features. There were two noticeable differences: (1) there was a considerable reduction in intensity of



SCOP- and CAC-related bands in the frequency ranges of 1200-1100 cm^{-1} and 1015-640 cm^{-1} , respectively, together with the peak at 3430 cm^{-1} . and (2) prominent new bands developed at 3300, 3100, 1070, 1040, 960, and 740 cm^{-1} . Furthermore, these spectral features were very similar to those of the $\text{NH}_4\text{H}_2\text{PO}_4$ -derived CPC specimens which was reported in our previous paper⁸. Hence, we can assume that the new bands at 3300, 3100, and 740 cm^{-1} can be ascribed to the formation of boehmite, $\gamma\text{-AlOOH}$, as the hydrothermal reaction product. The other reaction product was hydroxyapatite (HOAp), $\text{Ca}_5(\text{PO}_4)_3(\text{OH})$, corresponding to the new bands at 1070, 1040, and 960 cm^{-1} . The intensity of these new bands became stronger with a further increase in temperature to 300°C. By comparison with the Na-M-derived specimens, the spectra for the autoclaved Na-P specimens (not shown) expressed the fact that such reaction products had already formed in the CPC body at the low hydrothermal temperature of 100°C. As evident from the pronounced growth of IR absorption bands, treatments at 200°C and 300°C led to a well defined formation of HOAp and $\gamma\text{-AlOOH}$ reaction products.

To support the IR data, an XRD tracing, ranging from 0.356 to 0.249 nm, was made for the same specimens as those used in the IR analyses. The results are given in Figure 4. For the Na-M systems, the diffraction pattern of the 100°C-autoclaved specimens showed only the chemical components of non-reactive CAC, such as monocalcium aluminate, $\text{CaO} \cdot \text{Al}_2\text{O}_3$, (CA), gehlenite, $2\text{CaO} \cdot \text{Al}_2\text{O}_3 \cdot \text{SiO}_2$ (C_2AS) and monocalcium dialuminate, $\text{CaO} \cdot 2\text{Al}_2\text{O}_3$, (CA_2). There were dramatic changes in the diffraction patterns of the 200°C-autoclaved specimens; several new d-spacings had developed and the line intensities of the non-reactive CAC had decreased.

These new spacings reveal the formation of two different crystal phases, HOAp and $\gamma\text{-AlOOH}$. This result implicated hydrothermally catalyzed *in-situ* conversion of amorphous phases into a crystalline one: namely, the amorphous SCOP phase was transformed into HOAp crystals. For $\gamma\text{-AlOOH}$, we can assume that the acid-base reaction between the proton-donating NaH_2PO_4 and the Ca cations dissociated from CAC surfaces at room temperature may not only lead to the formation of SCOP salt, but also to the development of the $\text{Al}_2\text{O}_3 \cdot x\text{H}_2\text{O}$ gels caused by a progressive liberation of Al ions from the Ca-depleted CAC surfaces⁸. If this concept is correct, the $\text{Al}_2\text{O}_3 \cdot x\text{H}_2\text{O} \rightarrow \gamma\text{-AlOOH}$ phase transition might occur in hydrothermal environments at 200°C. Such hydrothermal-catalyzed phase

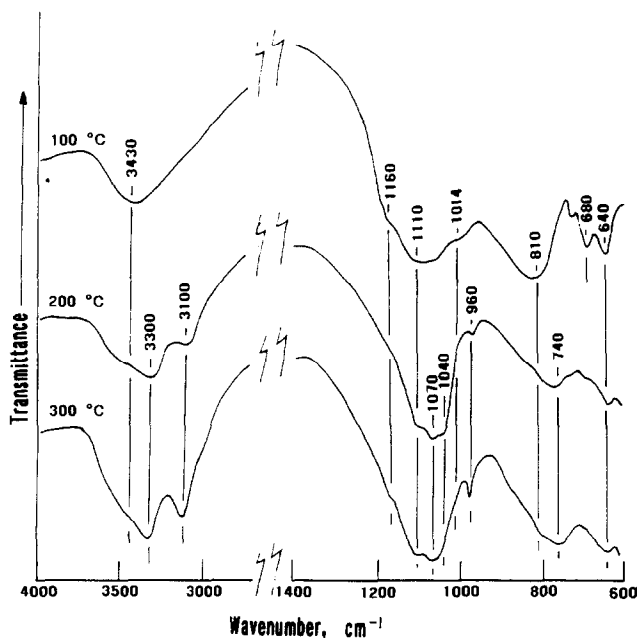


Figure 3. FT-IR spectra for Na-M-derived CPC specimens after exposure in autoclaved at 100, 200, and 300°C.

transformations, $\text{SCOP} \rightarrow \text{HOAp}$ and $\text{Al}_2\text{O}_3 \cdot x\text{H}_2\text{O} \rightarrow \gamma\text{-AlOOH}$, strongly suggest that even though the Na-based phosphates reactants substituted for the NH_4 -based phosphates, the resultant in-situ conversion mechanism is much the same as that of CPC derived from $\text{NH}_4\text{H}_2\text{PO}_4$ reactants. Comparing the heights of the spacings, the degree of crystallinity of these phases was enhanced with an increased hydrothermal temperature. At 300°C , these conversion products became the major phases, while there was a remarkable reduction in line intensity of CAC-related d-spacings. The reason for this reducing trend as a function of increasing temperature was the further promotion of the acid-base reaction between the residual CAC and NaH_2PO_4 by hydrothermal catalysis. Although some non-reactive CAC still remained in the body of the cement, a high rate of in-situ conversion into HOAp and $\gamma\text{-AlOOH}$ phases was observed in the XRD pattern of the Na-P-derived CPC specimens after exposure to the relatively low temperature of 100°C (see Figure 4). As expected, an increase in temperature caused further development of crystallinity of HOAp and $\gamma\text{-AlOOH}$, and a considerable reduction of the CAC reactant. Therefore, the high reactivity of Na-P with the CAC provided two major advantages: one was the introduction of an abundant SCOP salt reaction products responsible for the development of strength at room temperature into the CPC bodies, and the other was the promotion of amorphous-crystal ($\text{SCOP} \rightarrow \text{HOAp}$ and $\text{Al}_2\text{O}_3 \cdot x\text{H}_2\text{O} \rightarrow \gamma\text{-AlOOH}$) phase conversions at a low hydrothermal temperature.

This information was correlated directly with the changes in compressive strength and porosity for Na-M- and Na-P-derived CPC specimens after exposure for 24 hrs in autoclave at 100, 200, and 300°C . Three different concentrations, 20, 30, and 40 wt%, of these phosphate reactants were used. Figure 5 represents the compressive strength-temperature relation, and shows that the increase in strength of the autoclaved CPC specimens depended on the following three factors: (1) the concentration of phosphate reactants, (2) the species of phosphate family, and (3) the hydrothermal temperatures. Referring to the first factor, the incorporation of concentrated phosphate solution into the CAC strengthened the specimens. The second factor implied that the use of Na-P reactant contributed significantly to the increase in strength, compared with that of Na-M. The third

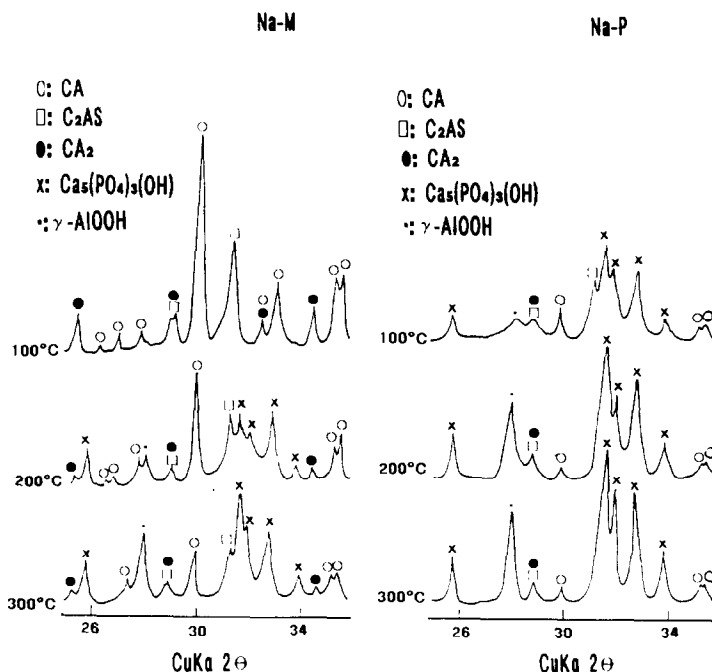


Figure 4. XRD patterns for 100-, 200-, and 300°C -autoclaved Na-P specimens.

factor reflected the fact that the hydrothermal treatment of CPC specimens made at room temperature significantly improved their strengths. Indeed, although there was no development of strength in the 40 and 30 wt% Na-M specimens made at 25°C, when exposed to 100°C, these specimens displayed a strength of > 20 MPa. For Na-P specimens, exposure at 200°C produced the highest strength; however, a further rise in temperature to 300°C reduced the strength. In contrast, the strength of autoclaved Na-M specimens increased at this temperature. Relating these findings to the *in-situ* phase transition, it seems that the ultimate development of strength in the autoclaved specimens probably is associated with the combined structure of the crystalline HOAp and γ -AlOOH phases, together with the amorphous $\text{NaCaPO}_4 \cdot x\text{H}_2\text{O}$ and Al_2O_3 gel phases which bind the partially reacted and non-reactive CAC particles into a coherent mass. An excessive *in-situ* growth of crystalline phases in the amorphous bodies, reflecting a high rate of amorphous \rightarrow crystal phase conversion, caused a decrease in strength.

Figure 6 plots the helium-induced porosity of autoclaved Na-M and Na-P specimens against temperature. Although the number of open pores for the Na-P bodies is much less than that for the Na-M specimens, the porosity for all the

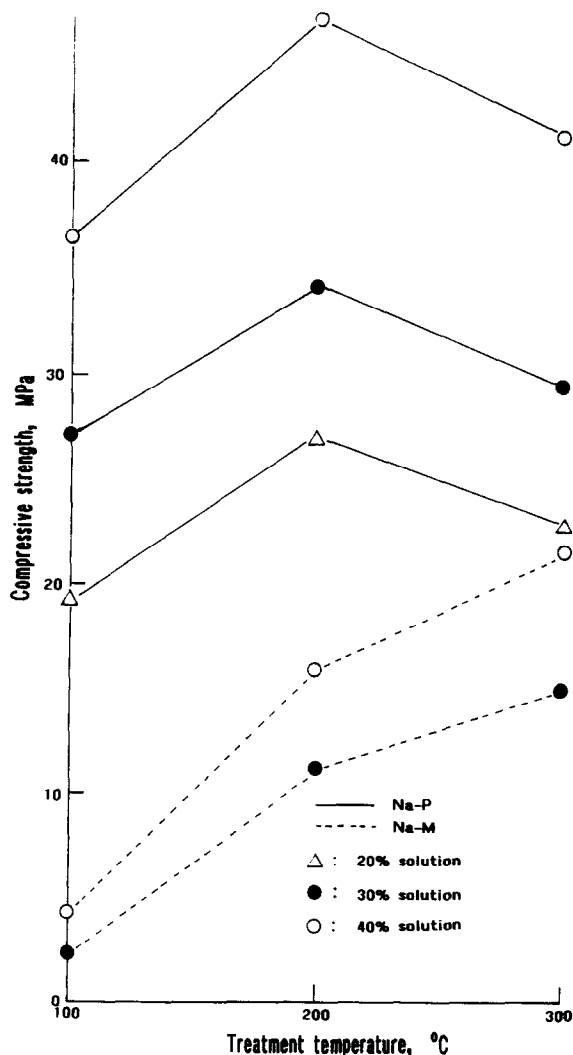


Figure 5. Changes in compressive strength of the Na-M- and Na-P-derived CPC specimens as a function of hydrothermal temperatures.

specimens tends to increase with increasing temperature. This information suggested that the increase in the rate of amorphous \rightarrow crystal conversion alters the porosity of the specimens. Nevertheless, the lowest number for porosity in these tests was obtained from the 40 wt% Na-P-derived CPC specimens, corresponding to their good mechanical behavior.

Lightweight CPC

With the information described above, we focused next on the characteristics of lightweight CPC (LCPC) specimens prepared from the low density slurries consisting of the Na-P solution, CAC powder, and aluminosilicate-hollow microsphere. The XRD pattern (not shown) for the "as-received" microspheres indicated that the major phase component of the shell of the spheres is mullite, $3\text{Al}_2\text{O}_3 \cdot 2\text{SiO}_2$. As discussed in the experimental section, the LCPC slurry was made up of the 40 wt% CAC, 20 wt% microspheres and 40 wt% Na-P solution. The Na-P solutions were 20, 30, and 40 wt% of Na-P solid in water, and the density of slurries deduced from their composition ranged from 1.25 to 1.28 g/cc. The characteristics to be investigated involved the water permeability, compressive strength, and alkali carbonation-resistance of 100-, 200-, and 300°C-autoclaved LCPC specimens. The water permeability was computed by the following formula:

$$K = \mu vl/APt$$

where K is the intrinsic permeability (darcys), μ is the fluid viscosity (cP), v refers to the volume (cm^3) of liquid flowing through a sample, during a time interval, l is the length (cm) of the sample, A corresponds to the cross-sectional area (cm^2), P is the hydraulic driving pressure (atm), and t is the time (sec) for the fixed volume of liquid to flow through sample under a given pressure gradient.

Table 2 summarizes the water permeability and compressive strength of autoclaved LCPC specimens. The table shows that an increase in the concentration of Na-P led to a low rate of water permeability and an improvement in strength. The data also indicated that 200°C was the most effective temperature in lowering water permeability and enhancing strength for all the specimens. An increase to 300°C increased the rate of water transportation through the specimens and caused a loss of strength, suggesting that a high rate of amorphous \rightarrow crystal phase conversion led to the formation of porous matrix layers in the LCPC. The 40 wt% Na-P-derived LCPC specimens, corresponding to a slurry density of 1.28 g/cc, had a water permeability ranging from 5.1×10^{-1} to 3.1×10^{-3} milli darcy, and a compressive strength of > 9.0 MPa, over temperatures of 100 to 300°C. In addition, we inspected the susceptibility of the 30 and 40 wt % Na-P-derived LCPC specimens to alkali carbonation by immersing for 10 days the 100-, 200-, and

Table 2. Changes in Water Permeability and Compressive Strength for 20, 30, and 40 wt% Na-P-Derived LCPC Specimens as a Function of Temperature

Concentration of Na-P, wt%	Hydrothermal Temperature, °C	Water permeability, milli darcy	Compressive strength, MPa
20	100	1.90	4.63
20	200	1.65	4.80
20	300	2.20	4.63
30	100	0.32	9.48
30	200	0.22	10.51
30	300	1.35	6.06
40	100	0.28	11.03
40	200	0.19	11.95
40	300	0.38	9.37

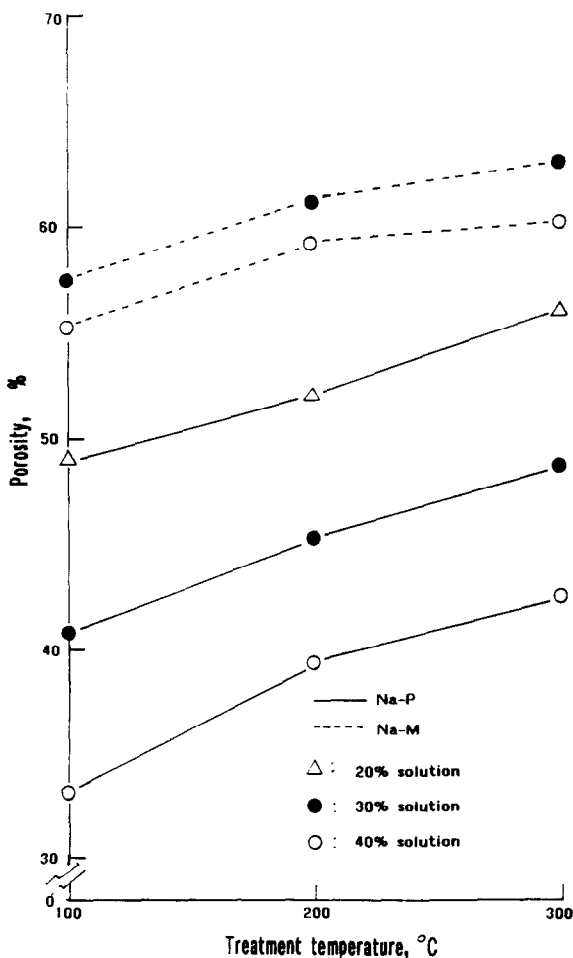


Figure 6. Porosity-temperature relation for autoclaved CPC specimens.

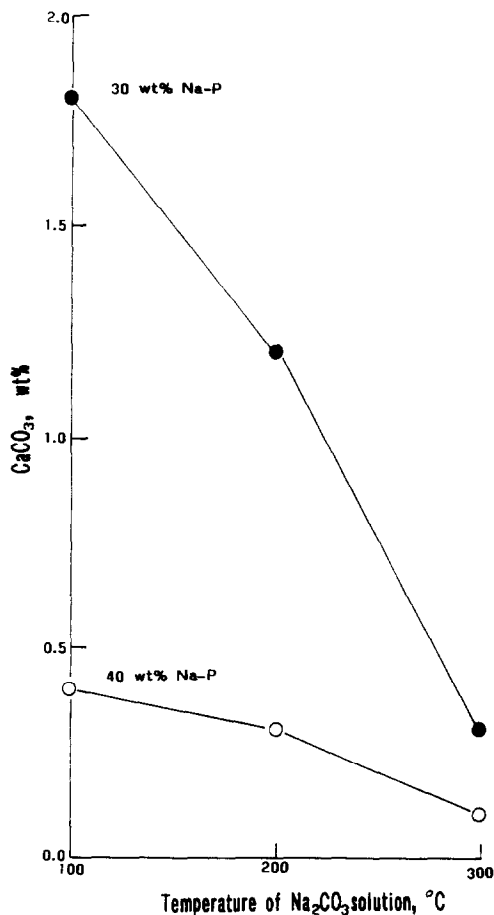


Figure 7. Concentration of CaCO_3 for 30 wt% and 40 wt% Na-P-derived LCPC specimens after exposure for 10 days to 0.05 M Na_2CO_3 solution at 100, 200, and 300°C.

300°C-autoclaved LCPC specimens for 10 days in 0.05 M Na_2CO_3 -laden water at temperatures of 100, 200, and 300°C. The amount of CaCO_3 present, reflecting the rate of carbonation, was determined from the specimen's weight loss at temperatures ranging from 600 to 770°C on the TGA curves. Figure 7 shows that the amount of CaCO_3 for both specimens decreases with an increase in the temperature of the Na_2CO_3 solution. This phenomenon is explicable from information reported in our previous paper²; namely, the major factor affecting carbonation of the autoclaved CPC specimens was the non-reactive CAC remaining in the CPC bodies. A large amount of residual CAC corresponded to a high production of CaCO_3 . As described earlier in IR and XRD studies, the elevated temperatures brought about a considerable elimination of residual CAC, while enhancing the rate of *in-situ* conversion into crystal HOAp and $\gamma\text{-AlOOH}$ which can be classified as a high CO_2 -resistance phase. Thus, we believe that a low concentration of CaCO_3 of < 0.5 wt% for specimens exposed in Na_2CO_3 solution at 300°C is due to the presence of a minimum amount of residual CAC, and well-formed HOAp and $\gamma\text{-AlOOH}$ phases in the CPC bodies.

Conclusions

We concluded that it is possible to use sodium phosphates [monobasic (NaH_2PO_4) or polybasic $\text{--}(\text{--NaPO}_3\text{--})_n$] as cement-forming solutions to replace ammonium phosphate solutions which are environmentally questionable, in preparing calcium phosphate cements (CPC) synthesized by the two-step, acid-base and hydrothermal reactions between the commercial calcium aluminate cements (CAC) as base reactant and phosphate solutions as the acid reactant. Considering the rate of acid-base reaction at ambient temperatures, we found that $\text{--}(\text{--NaPO}_3\text{--})_n$ reacted more favorably with the CAC than did NaH_2PO_4 , thereby resulting in a compressive strength of > 20 MPa and a porosity of $< 30\%$ for neat CPC pastes that were left for 24 hr at 25°C . In contrast, the strength of NaH_2PO_4 -derived CPC specimens was too low to be measured. The amorphous sodium calcium orthophosphate, $\text{NaCaPO}_4 \cdot x\text{H}_2\text{O}$ (SCOP) salts formed by the acid-base reaction were responsible for this development of strength. This reaction also led to the formation of $\text{Al}_2\text{O}_3 \cdot x\text{H}_2\text{O}$ gels on the surfaces of Ca-depleted CAC reactants. When these amorphous phases, which bind the partially reacted and non-reactive CAC particles into a coherent mass, were exposed in an autoclave at temperatures up to 300°C , the mechanisms of the phase conversion and transformation were essentially similar to those obtained from the $\text{NH}_4\text{H}_2\text{PO}_4$ -derived CAC specimens. Namely, the amorphous $\text{NaCaPO}_4 \cdot x\text{H}_2\text{O} \rightarrow$ crystalline hydroxyapatite, $\text{Ca}_5(\text{PO}_4)_3(\text{OH})$, (HOAp) and the amorphous $\text{Al}_2\text{O}_3 \cdot x\text{H}_2\text{O} \rightarrow$ crystalline γ -AlOOH phase transitions for the $\text{--}(\text{--NaPO}_3\text{--})_n$ -derived CPC specimens occurred at a hydrothermal temperature around 100°C , while the rate of acid-base reaction between residual CAC and Na phosphate was promoted by hydrothermal catalysis. Although an excessive rate of such in-situ amorphous \rightarrow crystal conversions caused a loss of strength and the development of porosity in the autoclaved CPC specimens, the formation of HOAp and γ -AlOOH phases, in conjunction with a minimum amount of non-reactive CAC in the CPC bodies, played a major role in inhibiting alkali carbonation of cements. In fact, the lightweight CPC specimens from the low-density slurry (1.28 g/cc) displayed a very low rate of carbonation, corresponding to a concentration of only 0.1% CaCO_3 after exposure for 10 days to $0.05 \text{ M Na}_2\text{CO}_3$ solution at 300°C .

References

1. T. Sugama and N.R. Carcillo, *Cem. Concr. Res.*, **22**, 783 (1992).
2. T. Sugama and N.R. Carcillo, *Cem. Concr. Res.*, **23**, 1409 (1993).
3. T. Sugama and E. Wetzal, "Microsphere-Filled Lightweight Calcium Phosphate Cements", *J. Mater. Sci.*, (in press).
4. W.W. Wedlandt, *Thermal Methods of Analysis*, 2nd Edn. p. 16, Wiley, New York (1974).
5. D.E.C. Corbridge and E.J. Lowe, *J. Chem. Soc.*, 493 (1954).
6. B.N. Nelson and G.J. Exarhos, *J. Chem. Phys.*, **71**, 2739 (1979).
7. L.J. Bellamy, *The Infrared Spectra of Complex Molecules*, 3rd Edn. p. 363, Chapman and Hall, London (1975).
8. T. Sugama, M. Allan and J.M. Hill, *J. Am. Ceram. Soc.*, **75**, 2076 (1992).